

A 3D discrete numerical elastic lattice method for seismic wave propagation in heterogeneous media with topography

Gareth S. O'Brien and Christopher J. Bean

Seismology and Computational Rock Physics Laboratory, Department of Geology, University College Dublin, Dublin, Ireland

Received 24 March 2004; revised 26 May 2004; accepted 22 June 2004; published 24 July 2004.

[1] A three-dimensional elastic lattice method for the simulation of seismic waves is presented. The model consists of particles arranged on a cubic lattice which interact through a central force term and a bond-bending force. Particle disturbances are followed through space by numerically solving their equations of motion. A vacuum free-surface boundary condition is implicit in the method. We demonstrate that a numerical implementation of the method is capable of modelling seismic wave propagation with complex topography. This is achieved by comparing the scheme against a finite-difference solution to the elastodynamic wave equation. The results indicate that the scheme offers an alternative 3D method for modelling wave propagation in the presence of strong topography and subsurface heterogeneity. We apply the method to seismic wave propagation on Mount Etna to illustrate its applicability in modelling a physical system. *INDEX TERMS*: 3210 Mathematical Geophysics: Modeling; 3230 Mathematical Geophysics: Numerical solutions; 7260 Seismology: Theory and modeling; 7255 Seismology: Surface waves and free oscillations. **Citation**: O'Brien, G. S., and C. J. Bean (2004), A 3D discrete numerical elastic lattice method for seismic wave propagation in heterogeneous media with topography, *Geophys. Res. Lett.*, *31*, L14608, doi:10.1029/2004GL020069.

1. Introduction

[2] Discrete particle methods have been successfully applied in physics for the past 30 years. They originate from solid-state physics models of crystalline materials [e.g., Hoover *et al.*, 1974]. These discrete methods do not solve continuum equations directly, for example the wave equation. Instead, they try to replicate the underlying physics at a 'microscopic scale' employing discrete micro-mechanical interaction rules between discrete material particles.

[3] The heterogeneous nature of geological materials leads to many challenges when modelling a variety of phenomena in natural structures. For example incorporating fractures, which can be non-welded interfaces, pore fluids and complex topography. The discontinuous nature of these natural flaws are often oversimplified in order to define a set of differential equations which can then be solved either analytically or numerically. As particle methods do not require continuum equations, they offer a possible means of incorporating this heterogeneity. In rock mechanics, discrete particle methods consist of particles, which represent blocks of intact rock, interacting through local radial and shear forces [Cundall and Strack, 1979]. This method-

ology has been used to model wave propagation [Toomey and Bean, 2000], tectonic processes [Saltzer and Pollard, 1992] and earthquake dynamics [Mora and Place, 1998]. The ability to incorporate highly heterogeneous materials is intrinsic to these schemes as they do not require special attention such as explicit boundary conditions.

[4] We describe a three dimensional discrete approach to modelling seismic wave propagation where we can include complex topography and arbitrary heterogeneity. In this paper we focus on dynamic deformation in the presence of topography. We outline the 3D discrete scheme, an elastic lattice method, (ELM), and validate the numerical scheme against a 4th order finite-difference solution to the elastodynamic wave equation. We also apply the method to seismic wave propagation on Mount Etna to illustrate its applicability in modelling a physical system.

2. Discrete Elastic Lattice Method

[5] Discrete particles methods have been successfully applied to seismic wave propagation in two dimensions. Toomey and Bean [2000] used a discrete particle scheme where the particles are arranged on a triangular lattice and interact through Hooke's Law (central-force term). Their method was restricted to a fixed Poisson's ratio of 0.25. del Valle-García and Sánchez-Sesma [2003] used a similar method, but included a bond-bending force term. The introduction of this force term, proportional to the angle between adjacent particles, enables the model to incorporate a variable Poisson's ratio. In this paper we outline a 3D ELM for wave propagation. The method is a 3D extension of the 2D elastic lattice method [Monette and Anderson, 1994]. Their method used square and triangular lattices to study the effects of brittle failure. In the 3D method, an elastic solid is represented by a series of interconnected springs arranged on a cubic lattice. We consider the model where each node has 18 neighbours, as shown in Figure 1. The elastic energy E_i for node i on the cubic lattice is expressed as [Arbabi and Sahimi, 1988]:

$$E_i = \frac{K}{2} \sum_{j=1}^{18} ([\mathbf{u}_{ij}] \cdot \mathbf{n}_{ij})^2 + \frac{c}{2} \sum_{jik} \left(\cos\theta_{jik} - \frac{1}{\sqrt{2}} \right)^2 \quad (1)$$

K is the elastic spring constant, c the bond-bending constant and θ_{jik} the angle between particles jik with node i as the apex of the angle. The displacement \mathbf{u}_{ij} is the displacement vector ($\mathbf{u}_i - \mathbf{u}_j$) and \mathbf{x}_{ij} is the vector connecting nodes \mathbf{x}_i and \mathbf{x}_j in the undistorted lattice and \mathbf{n}_{ij} is $\mathbf{x}_{ij}/|\mathbf{x}_{ij}|$. The first term is the central-force interaction summed over the 18 neighbours and the second term is the bond-bending term, which is summed over all angles jik . The energy density Φ is the total

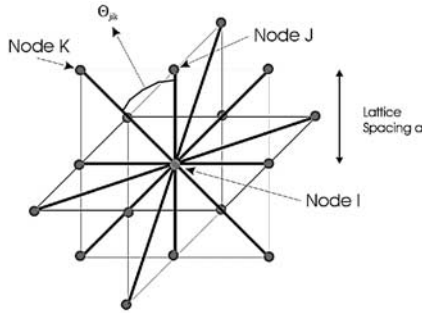


Figure 1. The medium is composed of particles that interact through Hooke's Law and a bond-bending force which is proportional to θ_{jik} , the angle between particles jik . The ELM in this study uses a cubic lattice with 18 neighbours, corresponding to the $[1\ 0\ 0]$ and $[1\ 1\ 0]$ lattice directions. See color version of this figure in the HTML.

energy stored in each spring divided by the total volume where a is the spacing between off diagonal nodes

$$\Phi = \frac{1}{a^3} \sum_{i=1}^N E_i \quad (2)$$

where N is the number of lattice nodes. Linearising equation (1) and substituting it into equation (2) gives

$$\Phi = \frac{1}{2a^3} \sum K \left(\frac{\mathbf{u}_{ij} \cdot \mathbf{x}_{ij}}{|\mathbf{x}_{ij}|^2} \right)^2 + \frac{1}{4a^3} \sum c \left(\frac{\mathbf{u}_{ij} \otimes \mathbf{x}_{ij}}{|\mathbf{x}_{ij}|^2} - \frac{\mathbf{u}_{ik} \otimes \mathbf{x}_{ik}}{|\mathbf{x}_{ik}|^2} \right)^2 \quad (3)$$

Expanding and rewriting this equation as a function of the strains gives

$$\Phi = \left(\frac{3K}{2a} + \frac{c}{a^3} \right) (\epsilon_{xx}^2 + \epsilon_{yy}^2 + \epsilon_{zz}^2) + \left(\frac{K}{a} - \frac{2c}{a^3} \right) (\epsilon_{xx}\epsilon_{yy} + \epsilon_{xx}\epsilon_{zz} + \epsilon_{yy}\epsilon_{zz}) + \left(\frac{2K}{a} + \frac{4c}{a^3} \right) (\epsilon_{xy}^2 + \epsilon_{xz}^2 + \epsilon_{yz}^2) \quad (4)$$

Comparing equation (4) with the elastic energy density of a 3D isotropic elastic continuum [Landau and Lifshitz, 1986] we can express the Lamé constants in terms of the spring and bond-bending constants.

$$\lambda = \frac{K}{a} - \frac{2c}{a^3} \quad (5)$$

$$\mu = \frac{K}{a} + \frac{2c}{a^3}$$

Thus, the elastic lattice method behaves as an elastic continuum where the elastic wave speeds are given by

$$v_p^2 = \frac{1}{\rho} \left(\frac{3K}{a} + \frac{2c}{a^3} \right) \quad (6)$$

$$v_s^2 = \frac{1}{\rho} \left(\frac{K}{a} + \frac{2c}{a^3} \right)$$

The force \mathbf{F}_{ij} on an individual node i from node j is given by

$$\mathbf{F}_{ij} = -K[(\mathbf{u}_i - \mathbf{u}_j) \cdot \mathbf{x}_{ij}] + \frac{c}{|\mathbf{x}_{ij}|^2} (\mathbf{u}_i - \mathbf{u}_j) \quad (7)$$

The force acting on each spring is calculated at each time step using equation (7) and the new position of the lattice

nodes and node velocities are updated using the velocity-Verlet numerical integration scheme [Allen and Tildesley, 1987]. This is a second-order in time and fourth order in space finite difference approximation to the equations of motion. The Velocity-Verlet integration scheme is symplectic and time reversible, which implies good stability. For numerical stability $\Delta t < a/V_{\max}$ where Δt is the time step and V_{\max} is the maximum compressional wave velocity. From the analysis of Toomey and Bean [2000], a minimum of 10 nodes per seismic wavelength are sufficient to avoid numerical dispersion. Heterogeneity can be incorporated into the model by changing the elastic spring constants on each spring. Topography is introduced by simply removing any particles above the required free surface. This imposes an implicit vacuum free-surface boundary condition. It also has the advantage that all the velocities and displacements are known on the free-surface hence velocity components need not be interpolated onto the free-surface, as is required with a staggered grid finite-difference method.

3. Comparison of ELM and Finite-Difference Method

[6] We compared the ELM to a finite-difference solution to the elastic wave equation. The finite-difference method is a fourth order in space and second order in time scheme from Ripperger *et al.* [2003]. The method is based on the staircase stacking method of Ohminato and Chouet [1997] where the Lamé constants λ and μ are set to zero above and on the free surface. Therefore the stresses are set to zero at these grid points. The free surface is discretised along certain planes so that the shear forces are only exposed at the surface or at horizontal or vertical edges. The normal stresses are embedded inside the medium. We follow this discretisation when we compare the two methods but it should be noted that this is unnecessary for the ELM, as we do not need to treat the free-surface explicitly.

[7] We used a homogeneous model with a Gaussian hill topography (Figure 2), the p-wave velocity is 4 km s^{-1} and the s-wave velocity is 2.5 km s^{-1} . The grid spacing is

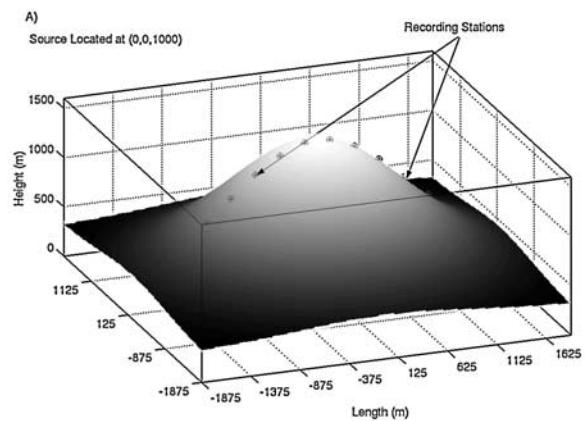


Figure 2. Gaussian hill topography with a homogeneous subsurface used in the ELM comparison with a finite-difference solution in the same model. The velocity seismograms were recorded on the free surface at the locations shown in the figure. See color version of this figure in the HTML.

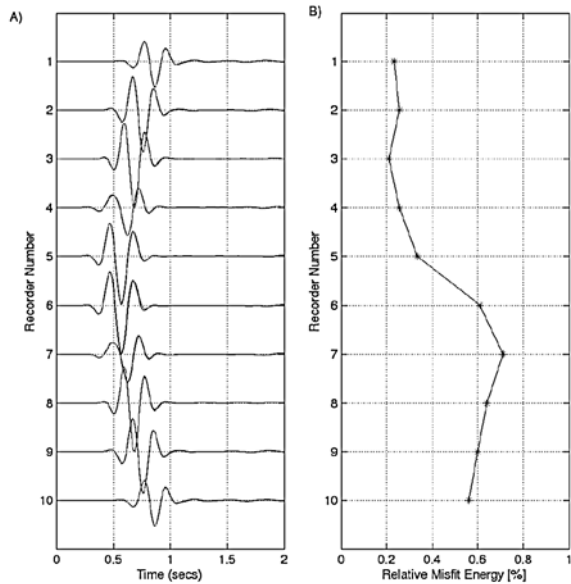


Figure 3. The ELM has been compared with a finite-difference (FD) solution to the elastic wave equation for dynamic deformation. The left panel shows a comparison of velocity seismograms (z-component), recorded on the profile shown in Figure 2, from a 5 Hz Ricker wavelet source (applied in the z-direction). The FD solution is the dashed line while the solid line is the elastic lattice model solution. The misfit energy between the two solutions is shown on the right hand panel, indicating a good fit between the methods. We found similar fits for the x- and y-components. Note: The misfit energy is calculated over the whole seismogram and includes small edge effects associated with non-perfect absorbing boundaries. See color version of this figure in the HTML.

12.5 meters with a time step of 0.001 seconds. A z-direction 5 Hz Ricker wavelet is used as the source function located in the center of the model, 625 m deep, Figure 2. We compare velocity seismograms along a profile shown in Figure 2. The finite-difference and elastic lattice method seismograms in Figure 3 have been normalised by their respective sources and then compared to one another. For each seismogram we computed the misfit energy ξ given by

$$\xi = \frac{\sum_{t=1}^T (S^{ELM}(t) - S^{FD}(t))^2}{\sum_{t=1}^T S^{FD}(t)^2} \quad (8)$$

where t is the time, $S^{FD}(t)$ is the finite-difference seismogram and $S^{ELM}(t)$ is the ELM seismogram. The seismograms are shown in Figure 3a while the misfit between the methods is shown in Figure 3b. In Figure 3a we can see visually that the seismograms are a close match and quantitatively they agree very well as seen in the misfit in Figure 3b. Both schemes were run on multiple processors and were computationally equivalent in both run time and memory requirements, given the same time step and grid spacing. Since a staggered grid fourth-order finite-difference method requires approximately 4 grid points per minimum wavelength, the ELM, which requires about 10 grid points,

requires more memory to avoid numerical dispersion. However, the method only requires the interaction of the nearest neighbour, which reduces the communication overheads for parallel computing.

4. Application to Rough Topography

[8] Pronounced topography is common in volcanic settings and plays an important role in distorting the recorded wavefield. The ELM is ideally suited to examining such topographical effects. A numerical experiment was per-

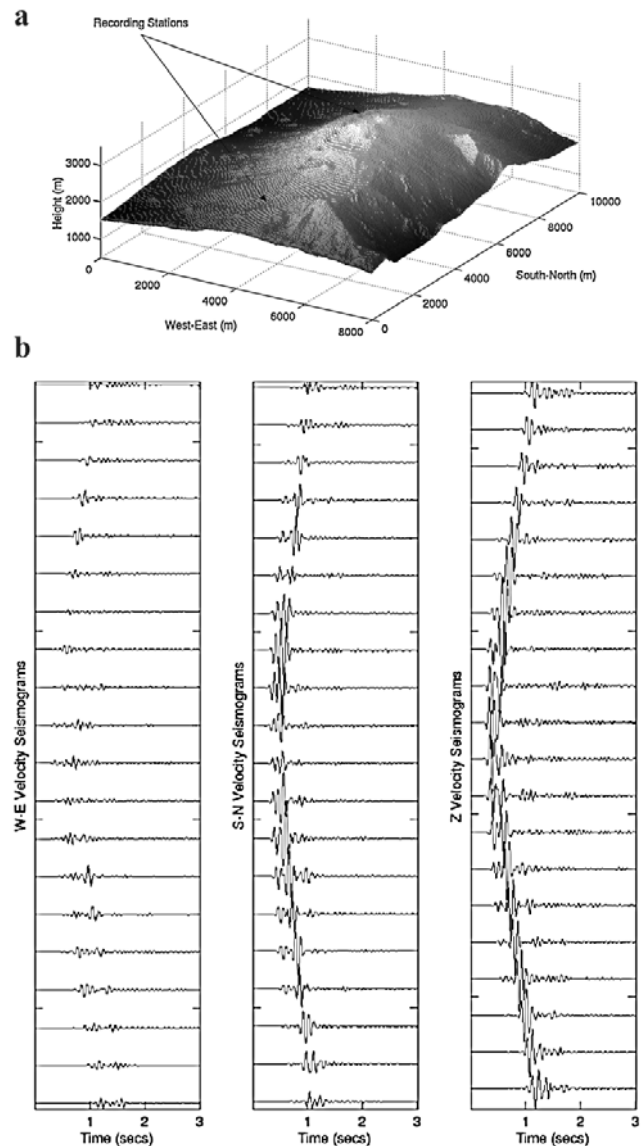


Figure 4. Top Panel: The digital elevation model of Mount Etna with a resolution of 20 m used in the simulation. The subsurface medium is homogeneous with $v_p = 4 \text{ km s}^{-1}$ $v_s = 2.3 \text{ km s}^{-1}$. Recorders were placed along a North-South profile as shown in the top panel. The most pronounced interface encountered by seismic waves is the free surface. The 3-component velocity seismograms clearly show the distortion of the initial Ricker wavelet source as a consequence of the complex topography. See color version of this figure in the HTML.

formed to illustrate the applicability of the elastic lattice method in examining such topographical effects. A digital elevation model, DEM, of Mount Etna with a grid spacing of 20 m was used in the simulation, Figure 4. The subsurface medium was homogeneous with a p-wave velocity of 4 km s^{-1} and the s-wave velocity was 2.3 km s^{-1} . Again, a 5 Hz Ricker wavelet was inputted as the source function in the z-direction located in the centre of the model at a height of 1.8 km. The 3-component velocity seismograms along a South-North profile are shown in Figure 4. Even for a simple homogeneous model the topography has a pronounced effect on the wavefield. By including external stresses, the ELM would also offer the possibility of examining static stress changes as a consequence of the deformation. This would allow one to model the seismic wavefield before and after a static deformation event.

5. Discussion and Conclusions

[9] The results show that the 3D elastic lattice method can be applied to seismic wave propagation including topography. The method is computational equivalent to a 4th order finite-difference method. The ELM has the added advantage that the wavefield is exactly known on the free surface and the topography does not need to be treated explicitly. The inclusion of heterogeneity is achieved by changing the elastic constants. Fracture discontinuities and porosity can be included by setting the elastic constants to zero. 2D discrete particle numerical simulations have shown non-linear wave propagation across fractures [Toomey *et al.*, 2002]. As discussed earlier we have focused only on dynamic deformation. Static deformation can be modelled by applying external forces to the model. Therefore, the method can be used to examine changes in the seismic wavefield as a consequence of static deformation, e.g., inflation/deflation in volcanic settings or 4D seismics. Elastic Lattice Methods offer an alternative approach to modelling wave propagation where several added features can be incorporated into numerical simulations.

[10] **Acknowledgments.** The authors acknowledge constructive comments by two reviewers that improved the clarity of the manuscript. We thank Gilberto Saccorotti for the Mt. Etna DEM. This work is funded by the Cosmogrid Ireland project, (funded under the Irish Government Programme for Research in Third Level Institutions).

References

- Allen, M. P., and D. J. Tildesley (1987), *Computer Simulations of Liquids*, Oxford Univ. Press, New York.
- Arbabi, S., and M. Sahimi (1988), Elastic properties of three-dimensional percolation networks with stretching and bond-bending forces, *Phys. Rev. B*, *38*, 7173–7176.
- Cundall, A., and O. Strack (1979), A discrete numerical model for granular assemblies, *Geotechnique*, *29*, 47–65.
- del Valle-García, R., and F. J. Sánchez-Sesma (2003), Rayleigh waves modeling using an elastic lattice model, *Geophys. Res. Lett.*, *30*(16), 1866, doi:10.1029/2003GL017600.
- Hoover, W. G., W. T. Arhurst, and R. J. Olness (1974), Two-dimensional studies of crystal stability and fluid viscosity, *J. Chem. Phys.*, *60*, 4043–4047.
- Landau, L. D., and E. M. Lifshitz (1986), *Theory of Elasticity*, Pergamon, New York.
- Monette, L., and M. P. Anderson (1994), Elastic and fracture properties of the two-dimensional triangular and square lattices, *Modell. Simul. Mater. Sci. Eng.*, *2*, 53–66.
- Mora, P., and D. Place (1998), Numerical simulation of earthquake faults with gouge: Towards a comprehensive explanation for the heat flow paradox, *J. Geophys. Res.*, *103*, 21,067–21,089.
- Ohminato, T., and B. A. Chouet (1997), A free surface boundary condition for including 3D topography in finite-difference method, *Bull. Seismol. Soc. Am.*, *87*, 494–515.
- Ripperger, J., H. Igel, and J. Wasserman (2003), Seismic wave simulation in the presence of real volcano topography, *J. Volcanol. Geotherm. Res.*, *128*, 31–44.
- Saltzer, S. D., and D. D. Pollard (1992), Distinct element modelling of structures formed in sedimentary overburden by extensional reactivation of basement normal faults, *Tectonics*, *11*, 165–174.
- Toomey, A., and C. J. Bean (2000), Numerical simulation of seismic waves using a discrete particle scheme, *Geophys. J. Int.*, *141*, 595–604.
- Toomey, A., C. J. Bean, and O. Scotti (2002), Fracture properties from seismic data—A numerical investigation, *Geophys. Res. Lett.*, *29*(4), 1050, doi:10.1029/2001GL013867.

C. J. Bean and G. S. O'Brien, Seismology and Computational Rock Physics Laboratory, Department of Geology, University College Dublin, Belfield, Dublin 4, Ireland. (gareth.obrien@ucd.ie)